Geoscience Frontiers 6 (2015) 277–284

HOSTED BY

ELSEVIER

Contents lists available at ScienceDirect

China University of Geosciences (Beijing)

Geoscience Frontiers

journal homepage: www.elsevier.com/locate/gsf

Research paper

Groundwater fluoride contamination: A reappraisal

Amlan Banerjee*

Geological Studies Unit, Indian Statistical Institute, Kolkata 700108, India

ARTICLE INFO

Article history:
Received 5 November 2013
Received in revised form
10 March 2014
Accepted 11 March 2014
Available online 22 March 2014

Keywords:
Fluoride
Contamination
Dissolution
Precipitation
Reactive–transport model

ABSTRACT

Dissolution of fluorite (CaF_2) and/or fluorapatite (FAP) [$Ca_5(PO_4)_3F$], pulled by calcite precipitation, is thought to be the dominant mechanism responsible for groundwater fluoride (F^-) contamination. Here, one dimensional reactive–transport models are developed to test this mechanism using the published dissolution and precipitation rate kinetics for the mineral pair FAP and calcite. Simulation results correctly show positive correlation between the aqueous concentrations of F^- and CO_3^{2-} and negative correlation between F^- and Ca^{2+}. Results also show that precipitation of calcite, contrary to the present understanding, slows down the FAP dissolution by 10^6 orders of magnitude compared to the FAP dissolution by hydrolysis. For appreciable amount of fluoride contamination rock–water interaction time must be long and of order 10^6 years.

1. Introduction

Groundwater fluoride concentration (>1.5 mg/L), according to WHO (1984) estimate, is affecting more than 260 million people around the world (Amini et al., 2008). Geographical areas with groundwater fluoride contamination are mostly characterized by the presence of crystalline basement rocks and/or volcanic bedrocks, arid–semi-arid climatic conditions, Ca^{2+} deficient $Na-HCO_3$ type groundwater (Handa, 1975; Rao, 1997; Saxena and Ahmed, 2001; Edmunds and Smedley, 2005; Sreedevi et al., 2006; Amini et al., 2008), long groundwater residence time, distance from the recharge area (Apambire et al., 1997; Genxu and Guodong, 2001; Jacks et al., 2005; Guo et al., 2007; Shaji et al., 2007), and happens predominantly by the weathering and dissolution of F^- bearing minerals (Handa, 1975; Rao, 1997; Genxu and Guodong, 2001; Saxena and Ahmed, 2001; Edmunds and Smedley, 2005; Jacks et al., 2005; Chae et al., 2006; Sreedevi et al., 2006; Guo et al., 2007). Though various minerals can be the potential geogenic sources of fluoride, fluorite and/or FAP has generally been considered as the dominant mineral phases for groundwater fluoride contamination (Handa, 1975; Nordstrom et al., 1989; Edmunds and Smedley, 2005; Chae et al., 2006; Reddy et al., 2010). Dissolution of fluorite (and FAP) can be enhanced by calcite precipitation that takes out Ca^{2+} from the solution by the following reaction

$$CaCO_3 + 2F^- + H^+ = CaF_2 + HCO_3^- \quad (1)$$

thus reducing the aqueous Ca^{2+} activity (Handa, 1975; Pickering, 1985; Nordstrom et al., 1989; Wenzel and Blum, 1992; Deshmukh et al., 1995; Saxena and Ahmed, 2001; Shah and Danishwar, 2003; Edmunds and Smedley, 2005; Jacks et al., 2005; Chae et al., 2006; Mamatha and Rao, 2010). The equilibrium constant of the reaction (1) is given as $K_{cal-fluor} = (a_{HCO_3^-})/[(a_{H^+})\cdot(a_{F^-})^2]$ (Handa, 1975) and shows that at a given pH, change in groundwater fluoride concentration is directly proportional to the change in bicarbonate concentration. Removal of Ca^{2+} can also be achieved by ion exchange (with Na^+) from clay minerals (Sarma and Rao, 1997) and thus changing the saturation state of the solution and increasing fluorite/FAP dissolution. Controlled laboratory experiments suggests that microbes can also influence groundwater fluoride contamination by dissolving minerals (like apatite, biotite, and feldspar containing trace phosphorous as apatite inclusions for nutrients) at a much faster rate and in the process release F^- (Taunton et al., 2000a, b; Hutchens et al., 2006; Welch et al., 2006) though field verification and the reaction rate kinetics for biogenic fluoride release is still lacking. Because of this it is beyond the scope of this work to quantitatively estimate biogenic groundwater fluoride release.

* Tel.: +91 3325752330.
E-mail addresses: amlanbanerje@gmail.com, amlanbanerji@yahoo.com.

Peer-review under responsibility of China University of Geosciences (Beijing)

1674-9871/$ – see front matter © 2015, China University of Geosciences (Beijing) and Peking University. Production and hosting by Elsevier B.V. All rights reserved.
http://dx.doi.org/10.1016/j.gsf.2014.03.003

However, to the author's knowledge, quantitative assessment of the dissolution mechanisms proposed for fluoride enrichment in natural waters (dissolution by hydrolysis, dissolution pulled by Ca^{2+} sink (calcite precipitation and/or ion exchange), and dissolution by microbial activity), especially through the study of fluid–mineral reaction kinetics are absent. Here, transient one dimensional reactive–transport models are developed, incorporating mineral reaction rates to quantitatively estimate fluoride enrichment in natural waters by (a) dissolution by hydrolysis and (b) dissolution pulled by carbonate precipitation mechanisms. FAP is selected as the representative fluoride bearing mineral, dissolution of which will release calcium and fluoride, and calcite as the representative carbonate mineral precipitation of which will sequestrate the released calcium and enhance FAP dissolution. FAP is selected over fluorite because the dissolution kinetics of fluorite (Zhang et al., 2006; Cama et al., 2010) is reported for extremely low pH range (1–3) which is off limit for the groundwater pH. Similarly for the carbonate minerals calcite is selected over dolomite because the kinetics of low temperature dolomite formation is still lacking.

2. Chemical reactions

Mechanism I: For the release of fluoride by FAP dissolution following reaction is considered

$$Ca_5(PO_4)_3F + 3H^+ = 5Ca^{2+} + 3HPO_4^{2-} + F^- \quad (2)$$

FAP dissolution for this scenario is decoupled from calcite precipitation.

Mechanism II: Reactions for calcite precipitation and FAP dissolution can be represented by

$$Ca^{2+} + CO_3^{2-} = CaCO_3 \quad (3)$$

$$Ca_5(PO_4)_3F + 3H^+ = 5Ca^{2+} + 3HPO_4^{2-} + F^- \quad (4)$$

Here, calcite precipitation (reaction (3)) and FAP dissolution (reaction (4)) are chemically coupled by Ca^{2+}. Calcite precipitation is triggering the dissolution of FAP by reducing the calcium activity of the solution. Combined mass balance equation relating the solute species in which groundwater is in contact with both calcite and FAP can given by

$$5CaCO_3 + 3HPO_4^{2-} + F^- = Ca_5(PO_4)_3F + 3H^+ + 5CO_3^{2-} \quad (5)$$

The equilibrium constant of this reaction (5) $K_{Cal-FAP} = (a_{H^+})^3\cdot(a_{CO_3^{2-}})^5/[(a_{HPO_4^{2-}})^3\cdot(a_{F^-})]$ resembles the equilibrium relationship between fluorite and calcite ($K_{cal-flour}$; Handa, 1975) and provides natural and independent control on groundwater calcium, fluoride, phosphate and carbonate composition. Precipitation of calcite is inhibited by the presence of dissolved magnesium, phosphate, iron and dissolved organic carbon (DOC) in the solution (Berner, 1975; Meyer, 1984; Walter, 1986; Lebron and Suarez, 1996). Here calcite precipitation is modelled using the inhibition effect of dissolved organic carbon only.

3. Quantitative method

3.1. Notation

ϕ = porosity.
c_i = concentration of aqueous species i (mol/L of pore volume).
c_i^{ic}, c_i^{bc} = initial and boundary concentrations of aqueous species i.
D = effective diffusion coefficient (cm^2/s).
U = velocity of water through pores (cm/s).
R_j = reaction rate of reaction j (mol/bulk $cm^3 s^{-1}$).
$\xi_{i,j}$ = stoichiometric coefficient of species i in reaction j, t = time (s) and x = length (cm).
k_{FAP} = rate constant of FAP dissolution reaction (2) (mol/cm^2 s^{-1}).
k_{CG} = precipitation rate constant due to calcite growth (mol/cm^2 s^{-1}).
k_{HN} = precipitation rate constant due to heterogeneous nucleation (mol/$cm^2 s^{-1}$).
S = surface area of mineral (cm^2/bulk cm^3).
K_{eq}^{FAP} = equilibrium constant for reaction (2).
K_{sp} = solubility product of pure calcite.
f(DOC) = function representing reduction of calcite precipitation due to dissolved organic carbon.
f(SA) = function of surface area of the suspended particles for heterogeneous nucleation.
Ω_{FAP} = saturation index of reaction (2). $\Omega > 1$ will trigger mineral precipitation, while $\Omega < 1$ will lead to its dissolution.
v_{FAP}, v_{cal} = volume fraction of FAP and calcite consumed and produced (cm^3 of mineral/bulk cm^3).
ρ_{FAP}, ρ_{cal} = molar density of FAP and calcite respectively (mol/cm^3 of mineral).

3.2. Reaction–transport equations

The process of FAP dissolution and calcite formation can be described by a set of continuity equations, coupled with mineral rate laws, change of volume, and initial and boundary conditions. For each species i in the system that take part in reaction j the continuity equation will be

$$\Gamma\phi\frac{\partial c_i}{\partial t} = \Gamma\phi D\frac{\partial^2 c_i}{\partial x^2} - \Gamma\phi U\frac{\partial c_i}{\partial x} + \sum_{j=1}^{n}\xi_{i,j}R_j \quad (6)$$

$\Gamma = 10^{-3}$ L/cm^3 appears because equilibrium constant values used here is consistent with mol/L but mineral reaction rates in mol/$cm^3 s^{-1}$ (Wang et al., 1995).

3.3. Mineral reaction rates

For each reaction involved in the reaction front, a basic linear rate law is adopted whereby rate is proportional to the thermodynamic affinity (Aagaard and Helgeson, 1982). For reactions (2) and (3) the affinity is proportional to $RT\ln Q$, where the supersaturation is $\Omega = Q/K_{eq}$ and the ion activity product $Q(=\prod_{i=1}^{k} c_i^n)$ is written in terms of all relevant aqueous concentrations, ensuring that all of them interact in the calculations. Assuming groundwater as a dilute solution (Fitts, 2012) all the activity coefficients getting into the rate equations are equal to 1, and molarity instead of molality units is used in all equations. The reaction rate for each of the individual reactions (FAP dissolution and calcite precipitation) (Lebron and Suarez, 1996; Harouiya et al., 2007) can be given as

$$R_{FAP} = k_{FAP}S(c_{H^+})^{0.6}(1-\Omega_{FAP}), \quad \text{where}$$
$$\Omega_{FAP} = \frac{(c_{Ca^{2+}})^5\cdot\left(c_{HPO_4^{2-}}\right)\cdot(c_{F^-})}{(c_{H^+})\cdot K_{eq}^{FAP}} \quad (7a)$$

and

Table 1
Values adopted in numerical simulations.

Variable	Symbol	Values adopted (unit) (references)
Concentration scale	C	10^{-8} (mol/L)
Diffusion coefficient	D	10^{-5}–10^{-6} (cm^2/s) (Wang et al., 1995)
Velocity	U	10^{-5}–10^{-6} (cm/s) (Wang et al., 1995)
Porosity	ϕ	0.1–0.01
Specific surface area	S_0	6–60 (cm^{-1}) (Wang et al., 1995)
Factor	L	10^{-3} (L/cm^3) (Banerjee and Merino, 2011)
FAP equilibrium constant	K_{eq}^{FAP}	$10^{-29.5}$–$10^{-29.9}$ (Harouiya et al., 2007)
Calcite solubility product	K_S^{cal}	4.8×10^{-9}
FAP rate constant	k_{FAP}^0	4×10^{-3} ($mol/cm^2\ s^{-1}$) (Harouiya et al., 2007)
Calcite rate constant	k_{cal}	10^{-11} ($mol/cm^2\ s^{-1}$) (Lebron and Suarez, 1996)
FAP molar density	ρ_{FAP}	0.0063 (mol/cm^3) (Guidry and Mackenzie, 2000)
Calcite molar density	ρ_{cal}	0.027 (mol/cm^3) (Banerjee and Merino, 2011)
Boundary FAP saturation	Ω_{FAP}^{bc}	0.002–0.1
Initial FAP saturation	Ω_{FAP}^{ic}	1.0
Boundary calcite saturation	Ω_{cal}^{bc}	2.3
Initial calcite saturation	Ω_{cal}^{ic}	1.0

$$k_{FAP} = k_{FAP}^0 \exp\left(-\frac{E_A}{RT}\right) \tag{7b}$$

and,

$$R_{cal} = k_{CG} S\left(c_{Ca^{2+}} c_{CO_3^{2-}} - K_{sp}\right) f(DOC)_{CG} + k_{HN} f(SA)(\log(\Omega - 2.5)) f(DOC)_{HN} \tag{8}$$

If, DOC $\geq$ 0.05 mM then,

$$R_{cal} = k_{HN} f(SA)(\log(\Omega - 2.5)) f(DOC)_{HN} \tag{9}$$

else,

$$R_{cal} = k_{CG} S\left(c_{Ca^{2+}} c_{CO_3^{2-}} - K_{sp}\right) f(DOC)_{CG} + k_{HN} f(SA)(\log(\Omega - 2.5)) f(DOC)_{HN} \tag{10}$$

3.4. Volume change

The change in mineral volumes of FAP and calcite due to dissolution and precipitation is expressed in the form

$$\frac{\partial v_{FAP}}{\partial t} = -\frac{R_{FAP}}{\rho_{FAP}} \tag{11}$$

and,

$$\frac{\partial v_{cal}}{\partial t} = \frac{R_{cal}}{\rho_{cal}} \tag{12}$$

Negative sign in Equation (11) represents FAP consumption.

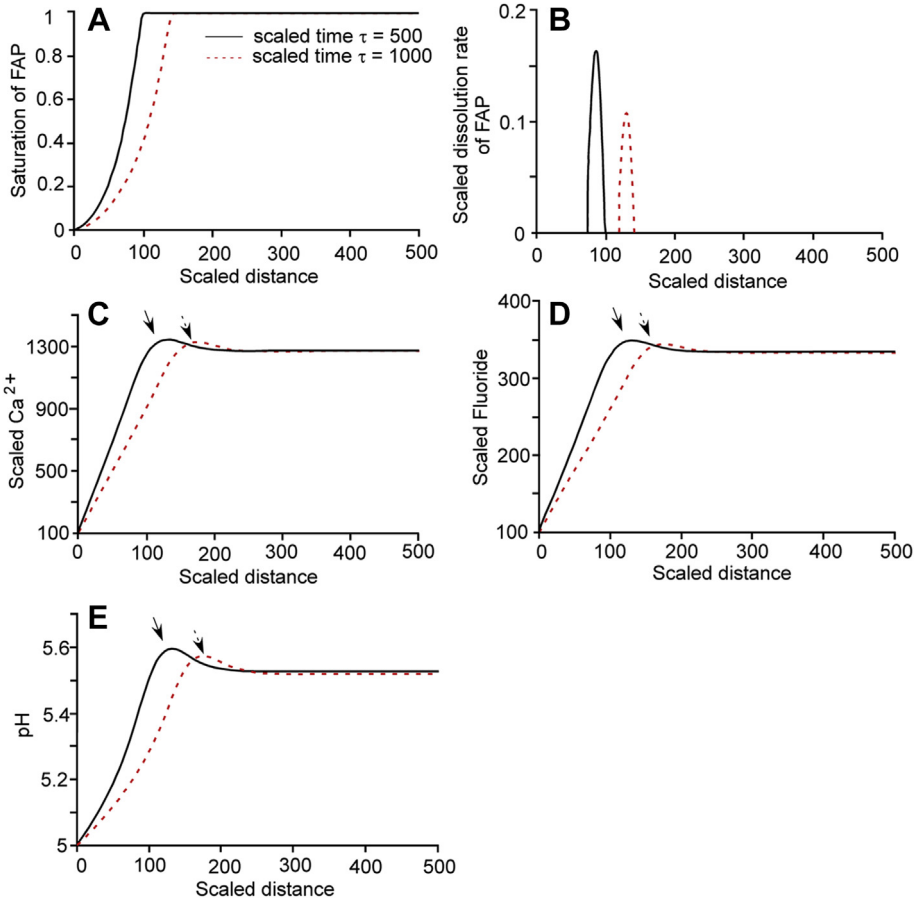

Figure 1. Results are shown for Mechanism I at two scaled time $\tau = 500$ (solid line) and $\tau = 1000$ (dashed line) units. (A) Calculated solution saturation profile with respect to FAP. Boundary FAP saturation value used for this simulation is 0.002 while the initial FAP saturation used is selected as 1.0. (B) Scaled FAP dissolution rate which gives the dissolution front velocity of 3.0496×10^{-5} cm/yr. The scaled concentrations of Ca^{2+}, F^- and solution pH are shown in figures (C), (D) and (E) respectively. Simulation results correctly present the release of the calcium and fluoride in the solution due to FAP dissolution and the consumption of H^+ that increases the solution pH (marked by arrows in the figures).

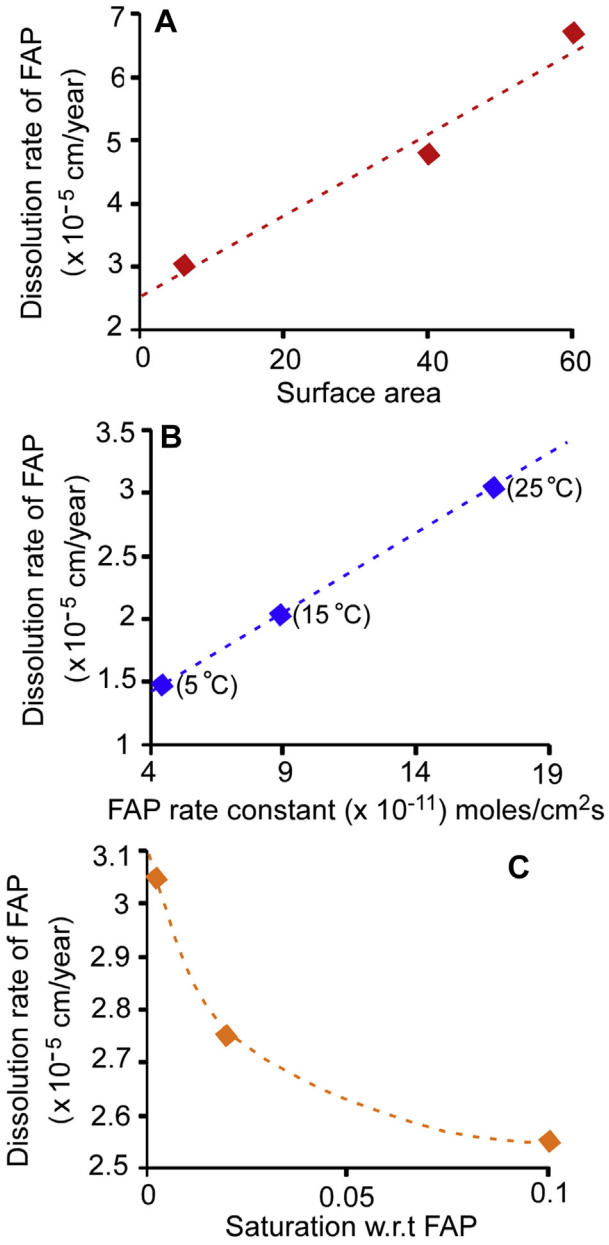

Figure 2. Dissolution front velocity (in cm/yr) as a function of reactive surface area (A), solution temperature (B) and solution saturation with respect to FAP (C).

3.5. Initial and boundary conditions

The initial and boundary conditions adopted in this study can be represented as

$$C(x, t = 0) \Rightarrow c_i^{ic} \tag{13}$$

$$\left.\begin{aligned} C(x = 0, t) &\Rightarrow c_i^{bc} \\ C(x = +\infty, t) &\Rightarrow \frac{\partial c_i}{\partial t} = 0 \end{aligned}\right\} \tag{14}$$

where c_i^{ic} and c_i^{bc} are initial and boundary concentrations of aqueous species *i*. The initial concentrations of the aqueous species are selected such that $\Omega_{FAP}^{initial} = 1.0$ and for the boundary condition at entry point $\Omega_{FAP}^{boundary}$ comes out as $<<1.0$. For calcite precipitation, concentration of the aqueous species are assigned such that $\Omega_{cal}^{initial} = 1.0$ but at the boundary the solution is slightly oversaturated with respect to calcite ($\Omega_{cal}^{boundary} \approx 2.3$).

The system of Equations (6)–(8), (11) and (12) are scaled (Wang et al., 1995; Banerjee and Merino, 2011) using time scale (*T*); length scale (*X*) and concentration scale (*C*) details of which is described in the Appendix I.

3.6. Calculation strategy

The scaled system of equations (*iv*, *vi* and *viii*; see Appendix I) using the scaled initial and boundary conditions (*xi*, *x*; see Appendix I) is solved using one dimensional implicit forward and central finite-difference scheme until the concentrations converge ($\leq 10^{-5}$). Each numerical simulation is a 'virtual experiment' of FAP dissolution and fluoride release yielding a set of profiles of aqueous concentrations, mineral modes, and reaction rates as functions of time and space.

3.7. Parameter choices

Many parameters enter into each simulation: temperature, advective velocity, diffusivity, porosity, surface area, rate constant, equilibrium constant, saturation of the aqueous solution with respect to FAP and calcite, dissolved organic carbon, imposed initial and boundary conditions, etc. Each parameter has been given values within a certain range (Table 1). The results are sensitivity experiments for a given set of parameters and the yield of reacted crystalline rock or the velocity of reacted front is compared.

4. Results

Mechanism I: Simulation results of FAP dissolution (by hydrolysis) at two scaled time slices $\tau = 500$ and $\tau = 1000$ are shown in Fig. 1. Time scale (*T*) and length scale (*L*) for this simulation come out as 2.851099×10^8 s and 2.99683×10^{-5} cm respectively. Simulations show that aqueous concentrations of Ca^{2+}, F^- and solution pH increase at the dissolution front (Fig. 1C, D, E marked by arrow) due to the dissolution of FAP by consumption of H^+. The solution saturation with respect to FAP (Fig. 1A) comes out <1.0 at and behind, and 1.0 ahead of the dissolution front, implying that FAP can only dissolve behind the dissolution reaction front. The transient profile of the scaled dissolution rate (Fig. 1B) shows that in a scaled time interval ($\Delta\tau$) of 500 units (=45.2 years) the FAP dissolution front migrates over a scaled length ($\Delta\lambda$) unit of 46 (=0.00138 cm), which gives the dissolution front velocity of 3.0496×10^{-5} cm/yr.

Dissolution of FAP is sensitive to the change in solution temperature and under − saturation with respect to FAP ($\Omega_{FAP} << 1$) (Fig. 2B, C). Decrease in groundwater temperature by five times (from 25 to 5 °C) decreases the FAP dissolution rate approximately by 2.08 times while decrease in under − saturation (from 0.002 to 0.1) decreases the rate of FAP dissolution by approximately 1.2 times. On the other hand increase in the reactive surface area FAP (from 6 to 60) increases the dissolution rate (Fig. 2A) by 2.2 times.

Mechanism II: Simulation results for the coupled FAP dissolution and calcite precipitation are shown in Fig. 3 for two scaled time slices $\tau = 500$ and $\tau = 1000$. The dissolution of FAP released Ca^{2+} in the solution and increases the solution supersaturation with respect to calcite from ~2.3 to 3.0 (Fig. 3A, B). Increase in supersaturation will lead to calcite precipitation that will sequestrate Ca^{2+} and thus lower the aqueous Ca^{2+} concentration and also the saturation index with respect to calcite which are reflected in the simulation results (marked by arrow in Fig. 3C, D and Fig. 3A, B) and

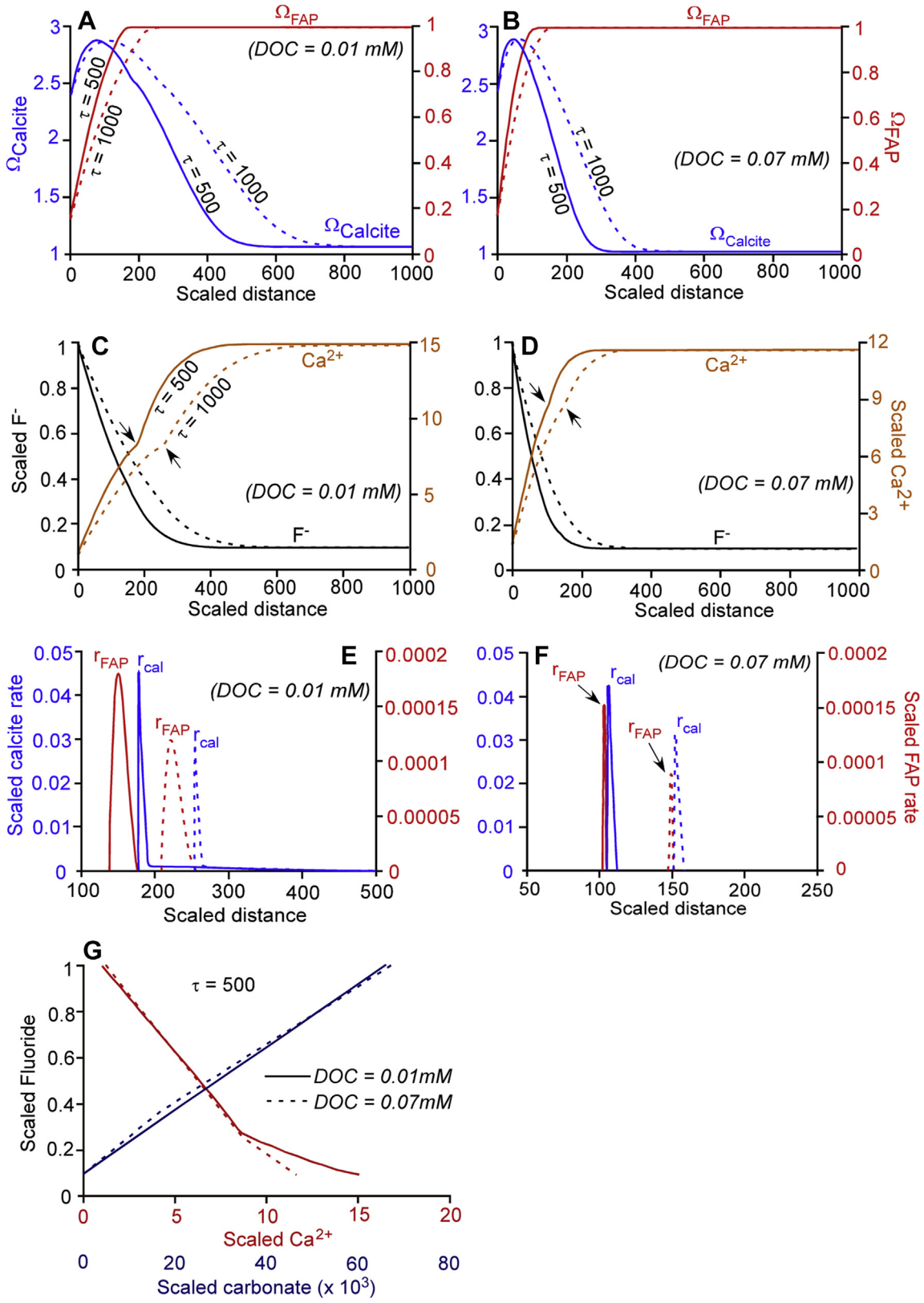

Figure 3. Results are shown for Mechanism II for two values of DOC concentration (0.01 mM and 0.07 mM) at two scaled time $\tau = 500$ and $\tau = 1000$ units. (A) and (B) show the calculated saturation profiles of FAP and calcite. Boundary saturation value used for FAP is 0.002 while the initial saturation used is 1.0. For calcite the boundary saturation is 2.3 while the initial saturation is 1.0. Profiles of Ca^{2+} and F^{-} are shown in (C) and (D). (E) and (F) show the scaled FAP dissolution and calcite precipitation rates. The FAP dissolution front velocity comes out extremely low, 6.14×10^{-11} cm/yr and 1.34×10^{-11} cm/yr for DOC = 0.01 mM and 0.07 mM respectively. Simulation results for this mechanism correctly represent the inversely proportional relationship of F^{-} and Ca^{2+} and directly proportional relationship of F^{-} and CO_3^{2-} (G).

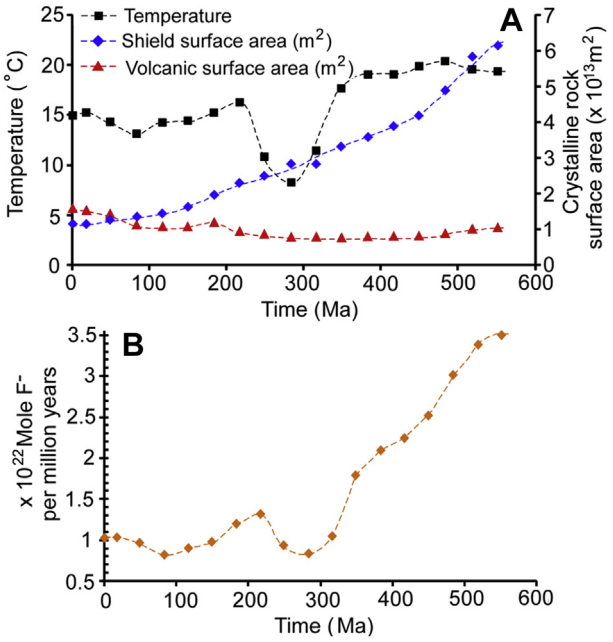

Figure 4. (A) Trends in global temperature and exposed igneous rock surface areas in the last 600 Ma (Phanerozoic) (adapted from Guidry and Mackenzie, 2000). Surface area available for weathering of shield rock decreases with time (from late to present) while that of volcanic rock remains roughly constant throughout. Temperature shows a declining trend (from late to present) and marked by dramatic climate change (from 20 to 8 °C) between 200 and 350 Ma. (B) Fluoride flux (of order 10^{22} mol F/Ma) released from the weathering of crystalline rocks at given temperatures over last 600 Ma. Equation (7) is used for FAP dissolution, solution saturation is selected as 0.002 and average weathering depth is selected as 100 cm.

coincides where the rate of calcite precipitation is maximum (Fig. 1E, F). Time scale (T) and length scale (L) for DOC = 0.01 mM come out as 4.166×10^9 s and 5.55×10^{-5} cm respectively; while for DOC = 0.07 mM it comes out as 3.42×10^{10} s and 1.6×10^{-4} cm respectively. The calculated FAP dissolution front velocity for DOC = 0.07 mM is of 1.34×10^{-11} cm/yr [in scaled time interval ($\Delta\tau$) of 500 units (=5.47×10^8 years) the dissolution–precipitation front migrates over a scaled length ($\Delta\lambda$) unit of 46 (=0.007 cm)] while for DOC = 0.01 mM it comes out as 6.2×10^{-11} cm/yr [in a scaled time interval ($\Delta\tau$) of 500 units (=6.14×10^7 years) the dissolution–precipitation front migrates over a scaled length unit ($\Delta\lambda$) of 73 (=0.004 cm)] implying that only 1.34–6.2 cm thick FAP will dissolve in 10^{11} years which is a very slow rate of mineral dissolution. This result also suggests that increase in inhibitor DOC concentration (from 0.01 to 0.07 mM) slows down the FAP dissolution rate by slowing down calcite precipitation. Simulation results also correctly show the positive correlation between the calculated aqueous concentrations of F^- and CO_3^{2-} and negative correlation between F^- and Ca^{2+} (Fig. 3G).

5. Discussion and conclusions

Release of fluoride in groundwater is attributed predominantly to the dissolution of fluoride rich minerals (notably fluorite and FAP). Transient one dimensional reactive–transport models are developed to quantitatively estimate groundwater fluoride enrichment by dissolution mechanisms. Simulation results demonstrate that calcite precipitation can indeed trigger FAP dissolution. Results correctly show that groundwater F^- concentration is directly proportional to CO_3^{2-} concentration and inversely proportional to Ca^{2+} (Fig. 3G). The correlation amongst F^-, Ca^{2+} and CO_3^{2-} can be explained by the following reaction $5CaCO_3 + 3HPO_4^{2-} + F^- = Ca_5(PO_4)_3F + 3H^+ + 5CO_3^{2-}$. Equilibrium constant for this reaction will be $K_{Cal-FAP} = (a_{H^+})^3 \cdot (a_{CO_3^{2-}})^5 / [(a_{HPO_4^{2-}})^3 \cdot (a_{F^-})]$, indicating that (at a given pH) any change in groundwater fluoride concentration is directly proportional to change in carbonate concentration and inversely proportional to the phosphate concentration. Inverse correlation of phosphate and fluoride is reported recently from Assam, India and Langtang area, Nigeria (Dutta et al., 2010; Dibal et al., 2012). One of the possible mechanisms of groundwater phosphate removal can be by the microbial activity which uses P as a nutrient required for construction of DNA, RNA, ADP, ATP, phospholipids, and polyphosphates (Taunton et al., 2000a,b; Hutchens et al., 2006; Welch et al., 2006). Results also show that the rate of FAP dissolution and release of F^- by the geochemical pull of calcite precipitation is extremely slow and FAP dissolves at a rate of 10^{-11} cm/yr. Addition of other inhibitors, like PO_4^{3-} and Fe^{2+} (Berner, 1975; Meyer, 1984; Walter, 1986; Lebron and Suarez, 1996) (not considered here) will further reduce the calcite precipitation and subsequent FAP dissolution and fluoride release.

On the other hand if FAP is dissolving only by hydrolysis, (i.e. FAP dissolution is decoupled from calcite precipitation), then FAP dissolution rate is of the order of 10^{-5} cm/yr which is 10^6 orders of magnitude faster than the coupled mechanism described above. Results also show that the release of fluoride by hydrolysis mechanism is proportional to the pH of the solution (Fig. 1D, E). Dissolution of FAP by hydrolysis is strongly dependent on temperature, reactive surface area and solution saturation state (Fig. 2A, B, C). For the decoupled FAP dissolution process using rate Equation (7), the calculated (following Guidry and Mackenzie, 2000) amount of total pre anthropogenic fluoride flux released from the crystalline rocks to the groundwater (as a function of time, temperature and available crystalline source rock) is shown in Fig. 4A, B. Results show that in the last 600 Ma fluoride flux is of the order of 10^{22} mol F^-/Ma and is decreasing with time due to the decrease in the available shield surface area and temperature as calculated by Bluth and Kump (1991) using published global depositional lithofacies maps and by Berner (1997) using GEOCARB II model.

Calculations proposed that for appreciable amount of fluoride contamination, rock–water interaction time must be greater than 10^6 years. This result corroborates well with the present understanding that fluoride concentration is proportional to the degree of water–rock interaction that enhances the dissolution of fluoride-bearing minerals in the rock (Nordstrom et al., 1989; Saxena and Ahmed, 2001; Chae et al., 2006), and is supported by the low solubility product of fluoride bearing minerals (example, fluorite solubility product is $10^{-10.57}$, Edmunds and Smedley, 2005) and slows mineral dissolution rates (calculated for minerals like fluorite and apatite, Chairat et al., 2007; Harouiya et al., 2007). Hence long groundwater residence time (in this study it comes out of order 10^6 years) is necessary for groundwater fluoride contamination. For example, Saxena and Ahmed (2001) put forward that the increase in fluoride concentration towards deeper wells can be attributed to the increase in groundwater residence time with increasing depth, which enhances the dissolution of fluorine-bearing minerals in rocks.

In summary, though both the mechanisms (dissolution by hydrolysis and dissolution pulled by calcite precipitation) can contribute to groundwater fluoride contamination, dissolution by hydrolysis is more efficient in releasing fluoride in groundwater. To buildup appreciable amount of fluoride concentration rock–water interaction time must be of order 10^6 years. Such groundwater is usually associated with deep aquifer systems and a slow groundwater movement. It is worth noting that the numerical solutions obtained using one

dimensional reactive – transport equations are dependent on mineral rate kinetics, temperature, reactive surface area and the saturation state of the groundwater with respect to calcite and FAP and the assumptions (like diffusivity, velocity, porosity) included in the model to arrive at a set of results, hence the results are not unique solutions.

Acknowledgements

The author acknowledge Dr. B. C. Raymahashay, Prof. S. Guha and an anonymous reviewer for their constructive comments that help to improve the manuscript.

Appendix I

Scaling of the equations

The system of Equations (6)–(8) are scaled using a time scale (T), length scale (X) and concentration scale (C) such that

$$\tau = \frac{t}{T},\ \lambda = \frac{x}{X},\ \text{and}\ \gamma_i = \frac{c_i}{C} \tag{i}$$

$$\text{where, time scale is defined as } T = \frac{\rho_j}{k_j S_o} \tag{ii}$$

$$\text{and, length scale is defined as } X = \left(\frac{\Gamma\phi DC}{k_j S_o}\right)^{0.5}. \tag{iii}$$

Concentration scale (C) is assigned a value of 10^{-4} mol/L, probably a typical order of magnitude of aqueous concentrations in the models.

After scaling, Equation (6) is converted into a pseudo – steady state equation of the form

$$\frac{\partial^2\gamma_i}{\partial\lambda^2} - \theta\frac{\partial\gamma_i}{\partial\lambda} + \sum_{i=1}^{n}\xi_{i,j}r_j = 0 \tag{iv}$$

$$\text{where, } \theta = \frac{\Gamma\phi UC}{k_j S_o X} = \frac{\Gamma\phi UCT}{\rho_j X} \tag{v}$$

and Equation (7) is converted in the form of

$$R_j = \eta_j r_j \tag{vi}$$

$$\text{where } \eta_j = k_j S_o,\ \text{and } r_j = \nu_j(\Omega_j - 1) \tag{vii}$$

and Equation (8) is represented in the form

$$\frac{\partial\nu_j}{\partial\tau} = r_j. \tag{viii}$$

The scaled *initial and boundary conditions* after scaling can be represented as

$$C(x, t = 0) \Rightarrow \gamma_i^{ic} \tag{ix}$$

$$\left.\begin{aligned} C(x = 0, t) &\Rightarrow \gamma_i^{bc} \\ C(x = +\infty, t) &\Rightarrow \frac{\partial\gamma_i}{\partial\tau} = 0 \end{aligned}\right\} \tag{x}$$

where γ_i^{ic} and γ_i^{bc} are scaled initial and boundary concentrations of aqueous species i.

Note that the self-consistent scaling results in a differential equation of mass conservation with only one parameter, θ, given by Equation (13), which combines many of the relevant individual parameters like infiltration velocity, porosity, concentration scale (C), length scale (L), and time scale (T).

References

Aagaard, P., Helgeson, H.C., 1982. Thermodynamic and kinetic constraints on reaction rates among minerals and aqueous solutions. I. Theoretical considerations. American Journal of Science 282, 237–285.

Amini, M., Mueller, K., Abbaspour, K.C., Rosenberg, T., Afyuni, M., Møller, K.N., Sarr, M., Johnson, C.A., 2008. Statistical modeling of global geogenic fluoride contamination in groundwaters. Environmental Science and Technology 42, 3662–3668.

Apambire, W.B., Boyle, D.R., Michel, F.A., 1997. Geochemistry, genesis, and health implications of fluoriferous ground waters in the upper regions of Ghana. Environmental Geology 33, 13–24.

Banerjee, A., Merino, E., 2011. Terra rossa genesis by replacement of limestone by kaolinite. III. Dynamic quantitative model. Journal of Geology 119, 259–274.

Berner, R.A., 1975. The role of magnesium ion in the crystal growth of calcite and aragonite from sea water. Geochimica et Cosmochimica Acta 39, 489–504.

Berner, R.A., 1997. The rise of plants and their effect on weathering and atmospheric CO_2. Science 276, 544–546.

Bluth, G.J., Kump, L.R., 1991. Phanerozoic paleogeology. American Journal of Science 291, 284–308.

Cama, J., Zhang, L., Soler, J.M., De Giudici, G., Ardvison, R.S., Luttge, A., 2010. Fluorite dissolution in acidic pH: in situ AFM and ex situ VSI experiments and Monte Carlo simulations. Geochimica et Cosmochimica Acta 74, 4298–4311.

Chairat, C., Schott, J., Oelkers, E.H., Lartigue, J.-E., Harouiya, N., 2007. Kinetics and mechanism of natural fluorapatite dissolution at 25°C and pH from 3 to 12. Geochimica et Cosmochimica Acta 71, 5901–5912.

Chae, G.T., Yun, S.T., Kwon, M.J., Kim, S.Y., Mayer, B., 2006. Batch dissolution of granite and biotite in water: implication for fluorine geochemistry in groundwater. Geochemical Journal 40, 95–102.

Deshmukh, A.N., Valadaskar, P.M., Malpe, D.B., 1995. Fluoride in environment: a review. Gondwana Geological Magazine 9, 1–20.

Dibal, H.U., Schoeneich, K., Garba, I., Lar, U.A., Bala, E.A., 2012. Occurrence of fluoride in the drinking waters of Langtang area, north central Nigeria. Health 4, 1116–1126.

Dutta, J., Nath, M., Chetia, M., Misra, A. Kr, 2010. Monitoring of fluoride concentration in groundwater of small tea gardens in Sonitpur district, Assam, India: correlation with physico-chemical parameters. International Journal of ChemTech Research 2, 1199–1208.

Edmunds, W.M., Smedley, P.L., 2005. Fluoride in natural waters. In: Selinus, O. (Ed.), Essentials of Medical Geology. Elsevier Academic Press, London, pp. 301–329.

Fitts, R.C., 2012. Groundwater Science. Elsevier Academic Press, London, pp. 692.

Genxu, W., Guodong, C., 2001. Fluoride distribution in water and the governing factors of environment in arid north-west China. Journal of the Arid Environment 49, 601–614.

Guidry, M.W., Mackenzie, F.T., 2000. Apatite weathering and the phanerozoic phosphorus cycle. Geology 28, 631–634.

Guo, Q., Wang, Y., Ma, T., Ma, R., 2007. Geochemical processes controlling the elevated fluoride concentrations in groundwaters of the Taiyuan Basin, Northern China. Journal of Geochemical Exploration 93, 1–12.

Handa, B.K., 1975. Geochemistry and genesis of fluoride- containing ground waters in India. Groundwater 13, 275–281.

Harouiya, N., Chaïrat, C., Köhler, S.J., Gout, R., Oelkers, E.H., 2007. The dissolution kinetics and apparent solubility of natural apatite in closed reactors ar temperatures from 5 to 50°C and pH from 1 to 6. Chemical Geology 244, 554–568.

Hutchens, E., Valsami-Jones, E., Harouiya, N., Chaırat, C., Oelkers, E.H., McEldoney, S., 2006. An experimental investigation of the effect of *Bacillus megaterium* on apatite dissolution. Geomicrobiology Journal 23, 177–182.

Jacks, G., Bhattacharya, P., Chaudhary, V., Singh, K.P., 2005. Controls on the genesis of some high-fluoride groundwaters in India. Applied Geochemistry 20, 221–228.

Lebron, I., Suarez, D.L., 1996. Calcite nucleation and precipitation kinetics as affected by dissolved organic matter at 25 °C and pH > 7.5. Geochimica et Cosmochimica Acta 60, 2765–2776.

Mamatha, P., Rao, S.M., 2010. Geochemistry of fluoride rich groundwater in Kolar and Tumkur districts of Karnataka. Environmental Earth Sciences 61, 131–142.

Meyer, H.J., 1984. The influence of impurities on the growth rate of calcite. Journal of Crystal Growth 66, 639–646.

Nordstrom, D.K., Ball, J.W., Donahoe, R.J., Whittemore, D., 1989. Groundwater chemistry and water–rock interactions at Stripa. Geochimica et Cosmochimica Acta 53, 1727–1740.

Pickering, W.F., 1985. The mobility of soluble fluoride in soils. Environmental Pollution Series B, Chemical and Physical 9, 281–308.

Rao, N.S., 1997. The occurrence and behaviour of fluoride in the groundwater of the Lower Vamsadhara river basin, India. Hydrological Sciences Journal 42, 877–892.

Reddy, D.V., Nagabhushanam, P., Sukhija, B.S., Reddy, A.G.S., Smedley, P.L., 2010. Fluoride dynamics in the granitic aquifer of the Wailapally watershed, Nalgonda district, India. Chemical Geology 269, 278–289.

Sarma, D.R.R., Rao, S.L.N., 1997. Fluoride concentrations in groundwaters of Visakhapatnam, India. Journal of Environmental Contamination and Toxicology 58, 241–247.

Saxena, V.K., Ahmed, S., 2001. Dissolution of fluoride in groundwater: a water–rock interaction study. Environmental Geology 40, 1084–1087.

Shah, M.T., Danishwar, S., 2003. Potential fluoride contamination in the drinking water of Naranji area, northwest frontier province, Pakistan. Environmental Geochemistry and Health 25, 475–481.

Shaji, E., Viju, B.J., Thambi, D.S., 2007. High fluoride in groundwater of Palghat District, Kerala. Current Science 92, 240–245.

Sreedevi, P.D., Ahmed, S., Made, B., Ledoux, E., Gandolfi, J.M., 2006. Association of hydrogeological factors in temporal variations of fluoride concentration in a crystalline aquifer in India. Environmental Geology 50, 1–11.

Taunton, A.E., Welch, S.A., Banfield, J.F., 2000a. Geomicrobiological controls on lanthanide distributions during granite weathering and soil formation. Journal of Alloys and Compounds 303, 30–36.

Taunton, A.E., Welch, S.A., Banfield, J.F., 2000b. Microbial controls on phosphate weathering and lanthanide distributions during granite weathering and soil formation. Chemical Geology 169, 371–382.

Walter, L.M., 1986. Relative efficiency of carbonate dissolution and precipitation during diagenesis: a progress report on the role of solution chemistry. In: Gautier, D.L. (Ed.), Roles of Organic Matter in Mineral Diagenesis, vol. 38. Society of Economic Paleontologists and Mineralogists Special Publication, pp. 1–12.

Wang, Y., Wang, Y., Merino, E., 1995. Dynamic weathering model: constraints required by coupled dissolution and replacement. Geochimica et Cosmochimica Acta 59, 1559–1570.

Welch, S.A., Taunton, A.E., Banfield, J.F., 2006. Effect of microorganisms and microbial metabolites on apatite dissolution. Geomicrobiology Journal 19, 343–367.

World Health Organization (WHO), 1984. Guidelines for Drinking Water Quality. In: Health Criteria and Other Supporting Information, vol. 2. World Health Organization, Geneva.

Wenzel, W.W., Blum, W.E.H., 1992. Fluoride speciation and mobility in fluoride contaminated soil and minerals. Soil Science 153, 357–364.

Zhang, R., Hu, S., Zhang, X., 2006. Experimental study of dissolution rates of fluorite in HCl-H_2O solutions. Aquatic Geochemistry 12, 123–159.